Simulation du comportement thermique du procédé d'enroulement filamentaire de composites thermoplastiques assisté par chauffage laser

Marta Perez, Anaïs Barasinski, Benoit Courtemanche, Chady Ghnatios, Emmanuelle Abisset-Chavanne, Francisco Chinesta

Simulation du comportement thermique du procédé d'enroulement filamentaire de composites thermoplastiques assisté par chauffage laser

Thermal simulation the laser-assisted tape placement process

M. Perez[1], A. Barasinski[1], B. Courtemanche[2], C. Ghnatios [3], E. Abisset-Chavanne[4] et F. Chinesta[4]

1 : GEM, UMR CNRS-Centrale Nantes
1 rue de la Noe, BP 92101, F-44321 Nantes Cedex 3, France
e-mail : marta.perez-miguel ;anais.barasinski@ec-nantes.fr

2 : CETIM - Technocampus Composites
ZI du Chaffault, Chemin du Chaffault, 44340 Bouguenais, France
e-mail : benoit.courtemanche@cetim.fr

3 : Notre Dame University Louaize
P.O. Box 72, Zouk Mikael, Zouk Mosbeh, Lebanon
e-mail : cghnatios@ndu.edu.lb

4 : ICI - High Performance Computing Institute, Ecole Centrale de Nantes
1 rue de la Noe, BP 92101, F-44321 Nantes Cedex 3, France
e-mail : emmanuelle.abisset-chavanne ;francisco.chinesta@ec-nantes.fr

Résumé

De nos jours, la production de grandes pièces en matériaux composites à matrice thermoplastique constitue un défi industriel complexe dès lors qu'il subsiste plusieurs difficultés liées à leur mise en forme. Le procédé de placement automatisé assisté par chauffage laser (LATP) est un procédé de fabrication conçu pour produire des pièces en composites thermoplastiques renforcés de fibres longues. Dans ce procédé, une bande est déposée et progressivement soudée sur un substrat, constitué des bandes préalablement déposées, grâce à un laser et un galet de compactage cylindrique. En ajoutant des couches successives, une pièce ayant la géométrie et les propriétés souhaitée est finalement produite. La mission principale de cette étude est de construire un modèle thermique dans lequel les paramètres d'entrée (géométriques ou matériaux) sont introduits, afin d'étudier leur influence sur la réponse thermique. Dans le cadre de la Décomposition Propre Généralisées (PGD) [3], les paramètres qui sont considérés comme des données d'entrée fixes avec les techniques de discrétisation classiques, peuvent être traités comme des coordonnées additionnelles du modèle. Ainsi, le champ inconnu est cherché sous une forme séparée, et par conséquent, une solution multidimensionnelle est obtenue. Finalement, cette approche va permettre d'analyser l'influence des paramètres d'entrée critiques sur la réponse thermique du modèle pendant le procédé.

Abstract

Nowadays, the production of large pieces made of thermoplastic composites is an industrial challenging issue as there are yet several difficulties associated to their processing. The laser-assisted tape placement (LATP) process is an automated manufacturing technique conceived to produce long-fibre reinforced thermoplastic matrix composites. In this process, a tape is placed and progressively welded on the substrate, consisting in the tapes previously placed, using a laser and a cylindrical compaction roller. By laying additional layers, a part with desired properties and geometry can be produced. The main task is to build a thermal model, where input (geometrical and material) parameters are introduced in order to study their influence on the thermal response. Within the Proper Generalized Decomposition framework [3], parameters considered as static input data in classical discretization techniques, can be introduced as extra-coordinates of the model. Thus, the unknown field is sought under a separated form hence a multidimensional solution is obtained. Finally, this will allow to analyze and establish the influence of the critical input parameters on the thermal response of the model during the process.

Mots Clés : Composites, Placement automatisé, Modèle thermique, Statistiques, Simulation stochastique
Keywords : Composites, Automated tape placement, Thermal modeling, Statistics, Stochastic simulation

1. Introduction

The context of this study is the LATP process, which is an automated filament winding process designed to produce composite parts with a thermoplastic matrix. A fiber-reinforced composite is

continuously laid-down onto the previously laid tapes around a mandrel, while the tape is heated up by the laser in order to bond it to the substrate. The objective is to strengthen this process in terms of reproducibility, control of parameters and control of manufacturing. Lot of experimental studies has been done and also numerical modelling regarding this process such as [4], [5], [1], [9], [6], [10]. Despite numerous analysis of process parameters some variability in the characteristics of the parts produced were still unexplained. A previous work [7] examined the state of the tape before the process and tried to relate temperature variations with the final quality of the parts. For this purpose, the tapes were analyzed by thermal cameras during the forming process also microscopic cross-sections of the tapes were done. The main objective of this work is to study the influence of material parameters variability into the thermal behaviour during the LATP process with the collected data of [7].

2. Characterization of the material and its variability

For this study, the material from two suppliers were chosen : Toho (TPUD PEEK HTS45 B12.7) and Suprem (55% AS4/PEEK−1500.15x12). Rings were manufactured consecutively and needed approximately 4.4 m of tape, which correspond about 6 tape thicknesses (Fig. 1). Two main information were provided to us from the previous work : temperature evolution measurements done with a thermal camera and microscopic cross-sections of the samples.

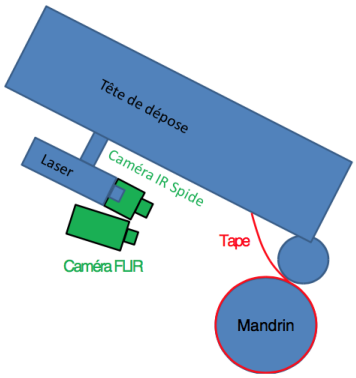

Fig. 1. Ring fabrication scheme.

The image analysis is used to observe the microstructure of the material to eventually define the actual properties based on the observation of the different phases. The analysis of these properties is then used to simulate composite manufacturing processes. This section addresses the characterization, as accurate as possible, of the material parameters from the microscopic cross-sections.The aim was to obtain information such as, fiber volume fraction (FVF), thickness or homogenized thermal conductivity tensor.

An active contour model was used in order to find the contour of the pre-impregnated (prepreg) composite. This method is based in an energy minimizing and requires the knowledge of the desired contour shape beforehand. This allowed to obtain a mask to detect the prepreg in the image. To detect the fiber in the image, the color image is converted to a gray-scale image. The gray scale image is then converted to a binary image based on a set threshold object detection method. The thresholding method replaces each pixel in an image with a black pixel if the image intensity $I(i, j)$ is less than some fixed constant $\mathcal{T}$. This was done for all the samples.

In [12] the size of a SRVE for a typical carbon fiber polymer is established and it is concluded that the minimum size is $\delta = \frac{L}{R} = 50$, being L the side of the element and R the fiber radius. This leads in our case, with a fiber diameter around 7 μm to a RVE whose size is equal to the thickness of the prepreg.

2.1. Fiber volume fraction

Fiber volume fraction (FVF) is the percentage of fiber volume in the entire volume of the fiber-reinforced composite material. For each microscopic cross-section, FVF was measured for 25 RVE in each microscopic cross-section of Suprem and Toho. For one RVE, the pixels whose value was equal to 1, that indicates a part of a fiber, were sum up and divided by all the pixels contained in the RVE leading to the obtainment of the fiber volume fraction. Fig. 2 plots the distribution of FVF for Suprem and Toho and gives a medium value of 46% in the case of Toho and 49% for Suprem.

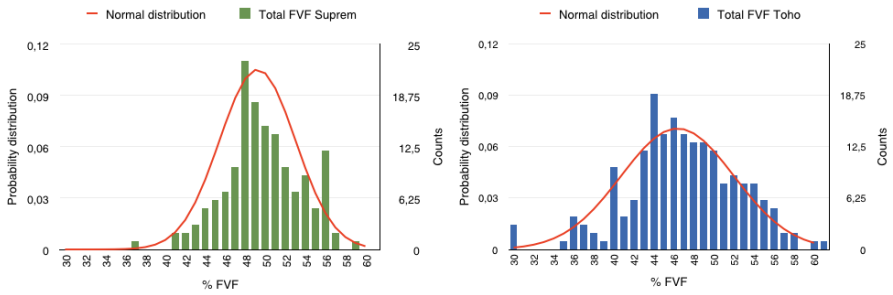

Fig. 2. Fiber volume fraction distribution for Suprem (green) and Toho (blue).

2.2. Thickness

The thickness was measured through y-axis (vertical direction of the image) and along the prepreg's width. results show important variations in the thickness in the case of Toho prepreg selected while for Suprem the thickness is more homogeneous. Figure 3 confirms this observations as the distribution of the thickness for all the Suprem samples are around 140 μm while for Toho data are more dispersed.

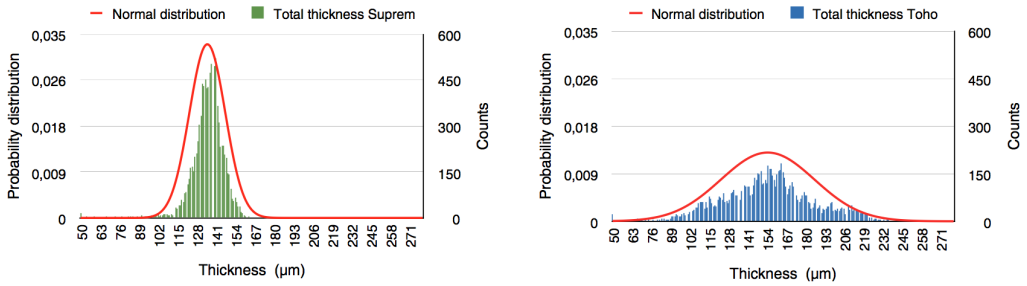

Fig. 3. Thickness distribution for Suprem (green) and Toho (blue).

2.3. Homogenized thermal conductivity

Due to microscopic heterogeneity the macroscopic thermal modeling needs a homogenized thermal conductivity that depends on the microscopic details. As detailed in [8], we can define the macroscopic temperature gradient ∇T at the RVE level from

$$\nabla T = \langle \mathbf{g}(\mathbf{x}) \rangle = \frac{1}{|\omega|} \int_{\omega} \mathbf{g}(\mathbf{x})\, d\mathbf{x}, \qquad \text{(Eq. 1)}$$

where $\mathbf{g}(\mathbf{x})$ denotes the microscopic temperature gradient. Following the homogenization theory, we assume the existence of a localization tensor $\mathbf{L}(\mathbf{x})$ relating the macroscopic temperature gradient ∇T with the microscopic local temperature gradient, such that

$$\mathbf{g}(\mathbf{x}) = \mathbf{L}(\mathbf{x}) \cdot \nabla T. \qquad \text{(Eq. 2)}$$

Now, we consider the microscopic heat flux $\mathbf{q}(\mathbf{x})$ according to the Fourier's law

$$\mathbf{q}(\mathbf{x}) = -\mathbf{k}(\mathbf{x}) \cdot \mathbf{g}(\mathbf{x}), \tag{Eq. 3}$$

and its macroscopic counterpart $\mathbf{Q}$ that is written

$$\mathbf{Q} = \langle \mathbf{q}(\mathbf{x}) \rangle = -\langle \mathbf{k}(\mathbf{x}) \cdot \mathbf{g}(\mathbf{x}) \rangle = -\langle \mathbf{k}(\mathbf{x}) \cdot \mathbf{L}(\mathbf{x},) \rangle \cdot \nabla T, \tag{Eq. 4}$$

from which the homogenized thermal conductivity can be defined from

$$\mathbf{K} = \langle \mathbf{k}(\mathbf{x}) \cdot \mathbf{L}(\mathbf{x}) \rangle. \tag{Eq. 5}$$

As $\mathbf{k}(\mathbf{x})$ is perfectly known everywhere in the RVE ω, the definition of the homogenized thermal conductivity tensor only requires the computation of the localization tensor $\mathbf{L}(\mathbf{x})$. We use essential boundary conditions on $\partial\omega$ corresponding to the assumption of uniform temperature gradient on the RVE ω. We consider the general 2D case that involves the solution of two boundary value problems related to the steady state heat transfer model in the microscopic domain ω for two different boundary conditions on $\partial\omega$:

$$\begin{cases} \nabla \cdot \left(\mathbf{k}(\mathbf{x}) \cdot \nabla \Theta^1(\mathbf{x}) \right) = 0 \\ \Theta^1(\mathbf{x} \in \partial\omega) = x \end{cases} \tag{Eq. 6}$$

and

$$\begin{cases} \nabla \cdot \left(\mathbf{k}(\mathbf{x}) \cdot \nabla \Theta^2(\mathbf{x}) \right) = 0 \\ \Theta^2(\mathbf{x} \in \partial\omega) = y \end{cases} . \tag{Eq. 7}$$

Thus, the localization tensor results finally :

$$\mathbf{L}(\mathbf{x}) = \left(\nabla \Theta^1(\mathbf{x}) \quad \nabla \Theta^2(\mathbf{x}) \right). \tag{Eq. 8}$$

To obtain the macroscopic homogenized thermal conductivity tensor we analyzed 150 microstructures in the case of Suprem and 196 for the Toho. The carbon fiber transverse conductivity [11] was set to $k_f = 0.8$ W/mK and the matrix conductivity $k_m = 0.2$ W/mK. All this leading to a thermal conductivity distribution along the width and the thickness as shown in Fig.4 and 5 respectively.

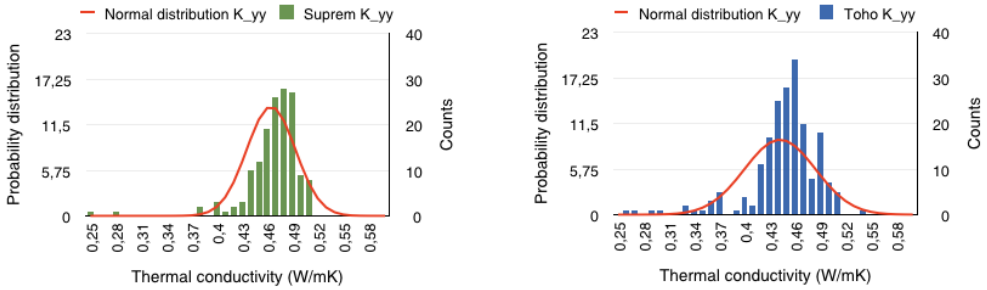

Fig. 4. Thermal conductivity along width direction distribution for Suprem (green) and Toho (blue).

2.4. Variability of the material

The main information extracted from the image analysis is listed in Table 1 and 2. This data will be the input parameters for the thermal model and the stochastic analysis developed in section 3 and section 4.

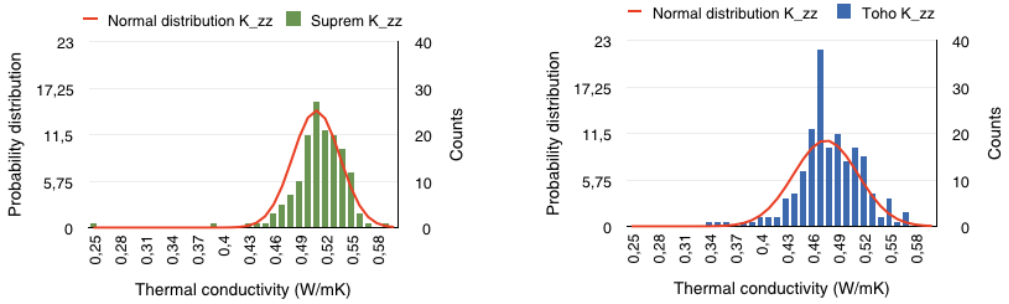

Fig. 5. Thermal conductivity along thickness direction distribution for Suprem (green) and Toho (blue).

Material parameters variability for Suprem			
Parameter	Mean, μ	Std dev, σ	μ/σ (%)
FVF (%)	49.2	3.79	7.7
Thickness (μm)	135.2	12.06	8.9
K_{yy} (W/mK)	0.465	0.029	6.2
K_{zz} (W/mK)	0.510	0.028	5.4

Tab. 1. Material parameters variablity for Suprem.

Material parameters variability for Toho			
Parameter	Mean, μ	Std dev, σ	μ/σ (%)
FVF (%)	46.4	5.64	12.2
Thickness (μm)	154.6	31.58	20.4
K_{yy} (W/mK)	0.442	0.042	9.5
K_{zz} (W/mK)	0.476	0.038	7.9

Tab. 2. Material parameters variablity for Toho.

3. Deterministic thermal model

The objective now is to obtain the steady state temperature in a coordinate system attached to the placement head, which is assumed to move with a constant velocity. For a given number of plies, this temperature field can be used to reconstruct the thermal history in any material point far enough from the edges. In these conditions each material point experiences the same thermal history during the process. It is progressively heated when approaching the laser, it reaches its maximum temperature when the laser applies directly on it and it cools down relatively fast when getting far from the heat source, reaching the ambient temperature before the laser comes back again when placing the next layer. Therefore, the laser and the roller are kept fixed and the material is assumed moving with a speed $\mathbf{v}$ in the opposite direction to the one in which laser and roller move. On the other hand, before experiencing the bonding the interface between the incoming layer and the substrate they cannot exchange heat through it.

The material domain, consisting in the substrate (plies already placed) and the incoming layer, in which Eq. 9 is solved is noted by $\Omega = [0, L_x] \times [0, L_y] \times [0, L_z]$. Within each ply the following heat problem is solved,

$$\rho C_p(\mathbf{v} \cdot \nabla T) = \nabla \cdot (\mathbf{K} \cdot \nabla T) \qquad \text{(Eq. 9)}$$

where T is the temperature, ρ is the density, C_p is the heat capacity, $\mathbf{K}$ is the anisotropic conductivity tensor and $\mathbf{v}$ is the velocity of the laminate with respect to the laser. The heating source is modeled as a surface flux. The boundary conditions are shown in Fig. 6, where the heat exchange conditions with

the air, roller and the mold, are introduced as follows

$$\mathbf{q}(\mathbf{x},t)\cdot\mathbf{n} = h_{air/composite}(T_{air} - T(\mathbf{x},t)) \qquad \text{(Eq. 10)}$$

where $\mathbf{q}$ is the heat flux, h is the heat transfer coefficient, T_{air} is the air temperature and $T(\mathbf{x},t)$ is the temperature of the point in the boundary.

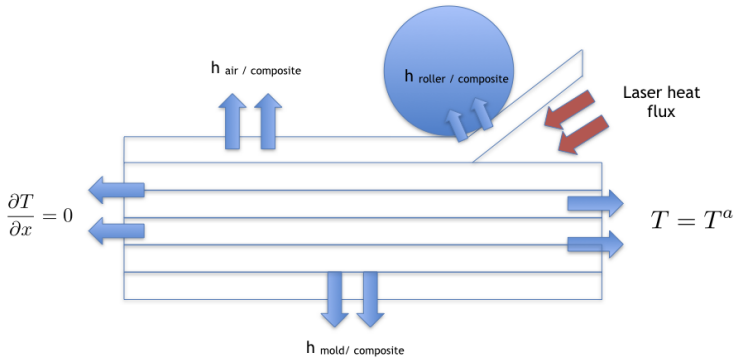

Fig. 6. Boundary conditions for the ring numerical simulation.

3.1. Proper Generalized Decomposition

In order to solve a single problem instead of one for each choice of the analyzed material parameters, we are going to introduce the material parameters as extra-coordinates in the thermal model. The difficulties related to the model's multidimensionality can be circumvented with a separated representation. The Proper Generalized Decomposition – PGD – [2] [3] is a discretization technique based on the use of separated representations in order to ensure that the complexity scales linearly with the model dimensionality. It consists of expressing the unknown field as a finite sum of functional products, i.e. expressing a generic multidimensional function $u(x_1,\cdots,x_d)$ as,

$$u(x_1,\cdots,x_d) \approx \sum_{i=1}^{i=N} X_i^1(x_1)\cdots X_i^d(x_d). \qquad \text{(Eq. 11)}$$

In the case of the thermal model presented above it involves as coordinates the space $\mathbf{x}$, the homogenized conductivity tensor $\mathbf{K}$, the thickness e and the parameter ρC_p. The simplest separated representation reads

$$T(\mathbf{x}, z, k_{yy}, k_{zz}, e, \rho C_p) \approx$$

$$\sum_{i=1}^{i=N} X_i(\mathbf{x})\cdot Z_i(z)\cdot K_i^{yy}(k_{yy})\cdot K_i^{zz}(k_{zz})\cdot E_i(e)\cdot R_i(\rho C_p) \qquad \text{(Eq. 12)}$$

that defines a problem defined in a high-dimensional space, that in the more general 3D case involves 7 dimensions but whose computational complexity is associated with the solution of some 2D related to the calculation of the function $X_i(\mathbf{x})$ and a series of 1D problems for calculating the remaining functions involved in Eq. 12.

3.2. Model validation

We consider $L_x = 1$ m and $L_y = 6$ mm. The velocity of the laminate is $\mathbf{v} = 0.12$ m/s and the power source $P = 1000$ W. The point of contact between the roller and the mandrel is placed at $x_r = 0.8$ m. The conductivity along the fiber direction is set to $K_{xx} = 5$ W/mK and the ambient temperature is considered $T^a = 22$ °C.

The composite specific heat capacity is calculated from the fiber volume fraction using the rule of mixtures as follows,

$$C_p = w_f C_{pf} + (1 - w_f) C_{pm} \quad \text{(Eq. 13)}$$

where w_f is the weight fraction of the fiber obtained from the image analysis. $C_{pf} = 1129$ J/kgK is the fiber specific heat capacity and $C_{pm} = 2200$ J/kgK is the specific heat capacity of the matrix. The values were chosen following the specifications of the suppliers.
The same is done for the composite density,

$$\rho = w_f \rho_f + (1 - w_f) \rho_m \quad \text{(Eq. 14)}$$

where $\rho_m = 1300$ kg/m^3 is the matrix density and $\rho_f = 1790$ kg/m^3 and $\rho_f = 1700$ kg/m^3 are the fiber density for Suprem and Toho, respectively.
Thus, a parametric solution is obtained with the material parameters – e, k_{yy}, k_{zz} and ρC_p – as extra-coordinates. Considering the mean values of the material parameters, the values of all transfers coefficients were fitted with the experimental measurements (i.e. for BT46) realized by [7]. This allowed to validate the model, in order to introduce the materials variability and study their influence on the thermal response (section 4).

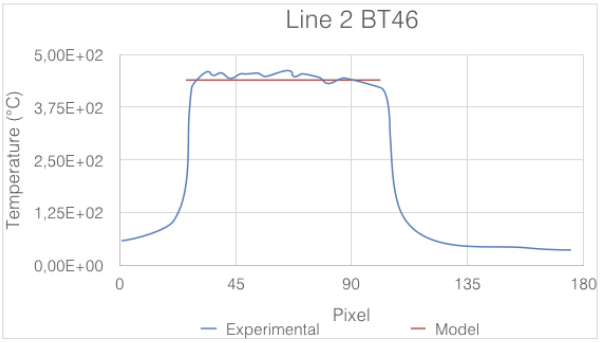

Fig. 7. Comparison between the experiment thermal measurements (blue) and the numerical model (red) for sample BT46.

4. Stochastic framework

The aim of this section is to quantify the material uncertainty. The stochastic simulation approach realized in this work is based in the Monte Carlo (MC) method. Monte Carlo simulation is a method for iteratively evaluating a deterministic model using sets of random numbers as inputs. By using random inputs, we are essentially turning the deterministic model into a stochastic model. Then the statistical characteristics of the model outputs are observed, and conclusions on them are drawn based on the statistical experiments.
In each numerical experiment, the possible values of the input random variables $\mathbf{X}(X_1, X_2, ..., X_n)$ are generated according to their distributions. Then the values of the output variable Y are calculated through the performance function $Y = g(\mathbf{X})$ at the samples of input random variables. With a number of numerical experiments carried out in this manner, a set of samples of output variable Y are available for the statistical analysis, which estimates the characteristics of the output variable Y.
The Monte Carlo method presents a robust but usually computational expensive method as N simulations must be generated. However, in this case, the advantage of the parametric solution is that the solution is already pre-calculated for the selected parameters, so, the computational expensive part is avoided.
Thus, $N = 10000$ numerical simulations were taken into account for the Monte Carlo analysis. The zone analyzed in the Monte Carlo is the zone were the thermal measurements were done in [7]. In the numerical simulation this corresponds to the volume $x \in [0.835, 0.855]$, $y \in [0.0024, 0.0036]$ and

$z = \frac{1}{4}e$. Results for only one value of temperature for each numerical simulation $i = 1, ..., N$ as the zone is averaged in order to visualize better the results. The input random variables – k_{yy}, k_{zz}, e and ρC_p – are generated according to the distributions shown in Table 1 and 2 for Suprem and Toho, respectively.

One Monte Carlo simulation was carried up for the Suprem material and another for the Toho material. In Table 3 different statistical results are given : sample mean, standard deviation, kurtosis and skewness. The histogram, as shown in Fig. 9, is a graphical representation of the distribution of numerical data and is an estimation of the probability distribution of a continuous variable (quantitative variable). Figure 8 shows more dispersion in the temperature results for the Toho material than for the Suprem material. Thus, for the same process conditions as the Toho material reaches higher temperature values this could lead to the degradation of the material while for the Suprem material not, although the mean values for both materials are similar as shown in Table 3.

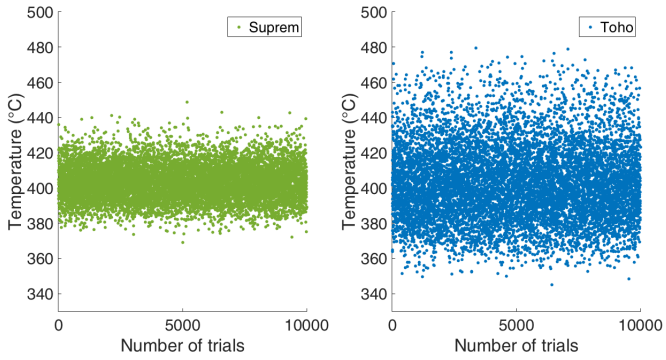

Fig. 8. Monte Carlo thermal simulations for ring setup.

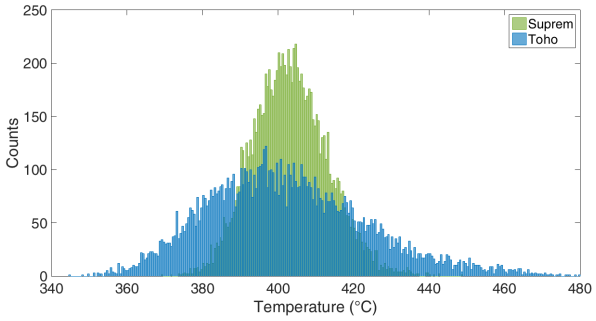

Fig. 9. Histograms for ring simulations.

Temperature (°C)		
Parameter	Suprem	Toho
Mean, μ	403.19	402.43
Std dev, σ	9.98	21.15
Kurtosis	3.13	3.12
Skewness	0.25	0.48

Tab. 3. Monte Carlo simulation results for ring setup.

Considering that, in the numerical simulation, $x = 0.8$ m is the contact point between the roller and the mandrel, the values from $x = 0.6$ to $x = 0.8$ m correspond to the consolidated tape and from $x = 0.8$ to 0.87 m the zone heated by the laser. Temperature values from the MC simulation are plotted along

the tape placement direction, from $x = 0.6$ to $x = 0.87$ m. The averaged temperature is shown with a solid line, the maximum temperature with a dashed line and the minimum with a dash-dotted line. Temperature results along the placement direction are given for the average value of temperature between values on the incoming tape and the substrate (Fig. 10 and 11).

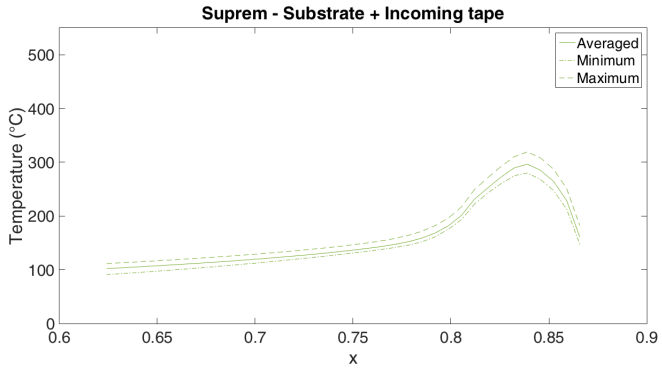

Fig. 10. Temperature averaged values along deposition direction (from right to left) of the incoming tape and the substrate for the ring setup.

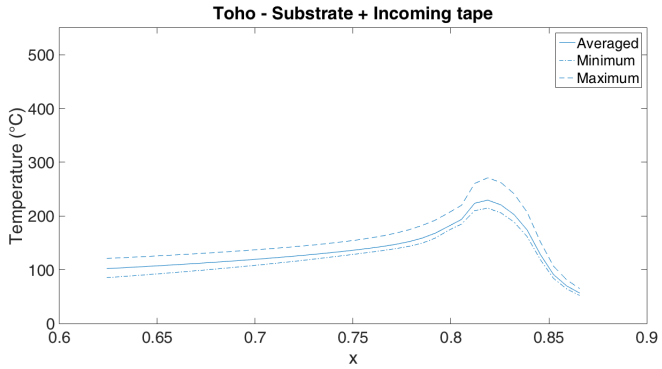

Fig. 11. Temperature averaged values along deposition direction (from right to left) of the incoming tape and the substrate for the ring setup.

In all the cases if we compare the Suprem material with the Toho material, there is more variability at the thermal response in the case of the Toho material, probably related to the heterogeneity of the material. It might be interesting to know which is the temperature gap desired at a control zone in order to obtain a good final part. This could allow us to give, for a fixed process parameters, the acceptable gap for the different material parameters in order to reach the desired temperature. However, all the previous information does not allow to say which is the material parameter that has more influence on the temperature values. For this, a sensibility analysis must be carried out.

5. Concluding remarks

The main objective of this work is to study of the influence of material parameters variability into the thermal behaviour during the LATP process with the collected data of [7]. In the case of the microscopic cross-sections, the data allowed to characterize the material variability for two different suppliers. The material parameters analyzed were the thickness, the fiber volume fraction (directly related to the parameter ρC_p in the numerical model) and the homogenized conductivity tensor in the cross-section of the tape (k_{yy} and k_{zz}). This characterization showed a higher variability for the Toho supplier than for the Suprem, which might have an influence on the thermal response.
On the other hand, the temperature measurements realized with the thermal camera allowed to validate our thermal simulation in order to extract information. However, most of experimental measurements

were done along the width of the tape in the hottest zone. It might be interesting to extend this measurements at different locations, i.e. near the contact between roller and mandrel, in order to better approach reality.
Once the simulation tool was validated, a stochastic approach based on Monte Carlo method was developed in order to quantify the material variability impact on the thermal response. Comparing both materials we have concluded more dispersion in the temperature values with the material with more variability (Toho). However, right now is not possible to conclude which material parameter has the greatest influence in the thermal response, thus a sensibility analysis must be carried out.
We can conclude that the results presented here show that material uncertainty can introduce significant variability in the thermal response with considerable cost implications in industrial practice. Consequently, variability effects should be incorporated in process design/optimization to address robustness. As perspectives, a deeper sensibility analysis could provide initial guesses for material parameters specifications. However, for this we should know which is the acceptable temperature range to ensure a good quality of the final part. After optimization, one could test how robust the model is to small changes in the values of the optimized parameters.

Références

[1] V. Agarwal. The role of molecular mobility in the consolidation and bonding of thermoplastic composite materials. PhD thesis, Delaware Univ., Newark, DE (United States), 1991.

[2] F. Chinesta, A. Ammar, E. Cueto. Recent advances and new challenges in the use of the Proper Generalized Decomposition for solving multidimensional models. Archives of Computational Methods in Engineering, **17/4**, 327-350, 2010.

[3] F. Chinesta, R. Keunings, A. Leygue. The Proper Generalized Decomposition for advanced numerical simulations. A primer. Springerbriefs, Springer, 2014.

[4] S. Grove. Thermal modelling of tape laying continuous carbon fiber reinforced thermoplastic. Composites, **19/5**, 367-375., 1988.

[5] S. Grove, D.Short. Evaluation of carbon fiber reinforced peek composites manufactured by continuous local welding of prepeg tape. Plastics and Rubber processing and applications, **10/1**, 35-44, 1988.

[6] W. Grouve. Weld Strengh of laser-assisted tape-placed thermoplastic composites. PhD thesis, University of Twente, 2012.

[7] K. Fouyer. Etude de la variabilité des caractéristiques thermiques des tapes de pré-imprégnés dans le cadre de l'enroulement filamentaire thermoplastique. Memoire de stage du Mastere specialisé, École Centrale de Nantes, 2016.

[8] E. Lopez, E. Abisset-Chavanne, F. Lebel R. Upadhyay, S. Comas, C. Binetruy, F. Chinesta. Advanced thermal simulation of processes involving materials exhibiting fina-scale microstructures. International Journal in Material Forming, 2015.

[9] R. Schledjewski, M.Latrille. Processing of unidirectional fiber reinforced tapes - fundamentals on the way to a process simulation tool (ProSimFRT). Composites Science and Technology, **63**, 2111-2118, 2003.

[10] CM. Stokes-Griffin, P. Compston, TI. Matuszyk, MJ. Cardew-Hall. Thermal modelling of the laser-assisted thermoplastic tape placement process. Journal Thermoplastic Composite Materials, 2015.

[11] T. Tian. Anisotropic thermal property measurements of carbon-fiber/epoxy composite materials. PhD thesis, 2011.

[12] D. Trias, J. Costa, A. Turon, J.E. Hurtad. Determination of the critical size of a statistical representative volume element (SRVE) for carbon reinforced polymers. Acta Materialia, **50**, 2006.